energies

MDPI

Article

Energy Savings Potential of Semitransparent Photovoltaic Skylights under Different Climate Conditions in China

Li Zhu [1,2], Peng Wang [1], Yujiao Huo [1,2,*], Wei Tian [3], Yong Sun [1,2] and Baoquan Yin [1,2]

[1] School of Architecture, Tianjin University, Tianjin 300072, China; zhuli1977@tju.edu.cn (L.Z.); pwangtju@163.com (P.W.); yong.sun@tju.edu.cn (Y.S.); yinbaoquan@tju.edu.cn (B.Y.)
[2] APEC Sustainable Energy Center, Asia-Pacific Economic Cooperation (APEC)/National Energy Administration (NEA) of China, Tianjin 300072, China
[3] School of Mechanical Engineering, Tianjin University of Science & Technology, Tianjin 300222, China; tjtianjin@gmail.com
* Correspondence: yujiaohuo@tju.edu.cn

Abstract: Due to the limited available envelope area, height-constrained buildings integrated with photovoltaics require that more attention be given to the effective use of roofs. Thus, it is crucial to study the energy savings potential of previously neglected semitransparent photovoltaic (STPV) skylights. In this paper, the net energy consumption (NEC) of a room with STPV skylights and energy superiority compared to a reference window were investigated. The energy savings potential was then calculated for five representative cases located in different climate zones and daylight zones, according to the mandatory codes to be implemented in April 2022. Through a global sensitivity analysis, the extent to which each component of the NEC affects the energy savings potential was evaluated. The results indicate that STPV skylights exhibit promising energy savings potential in China. In temperate zones with excellent daylight conditions, an energy savings potential of 0.21 to 2.55 can be achieved, while the maximum energy savings rate (ESR) for the other four cases ranges from 0.52 to 1.1. The effect of electricity power generation (EPG) on the energy savings potential is most pronounced, except for that of STPV skylights on sloped roofs in hot summer and cold winter zones with poor daylight.

Keywords: semitransparent photovoltaic (STPV); buildings integrated with photovoltaic; energy savings potential; global sensitivity analysis

Citation: Zhu, L.; Wang, P.; Huo, Y.; Tian, W.; Sun, Y.; Yin, B. Energy Savings Potential of Semitransparent Photovoltaic Skylights under Different Climate Conditions in China. *Energies* **2022**, *15*, 2358. https://doi.org/10.3390/en15072358

Academic Editor: Alessandro Cannavale

Received: 18 February 2022
Accepted: 21 March 2022
Published: 24 March 2022

1. Introduction

Building-integrated photovoltaic (BIPV) technology has been considered a practical and promising candidate for improving energy efficiency in buildings, as it combines energy production with other functions of the building envelope [1,2]. It has been demonstrated that semitransparent photovoltaic (STPV) envelopes exhibit higher energy efficiency than opaque envelopes [3]. Meanwhile, technological innovations have strongly promoted the application of STPV technology [4,5]. Since these new power production envelopes play a crucial role in energy performance for the heating, cooling, and lighting of buildings [6], they must receive more attention as emerging building materials [7,8].

The energy performance of building-integrated STPVs is influenced by numerous factors [9]. The visible light transmittance (VLT), solar heat gain coefficient (SHGC), and overall heat transfer coefficient (U-value) characterize the thermal performance of STPVs as a light-transmitting envelope [10]. The SHGC of an STPV facade was significantly reduced for incidence angles above 45° compared to SHGC for an incidence angle of 0° in the tropics [11]. Based on the data from five CdTe-based STPV modules with VLT values from 7.0% to 32.7%, the photovoltaic power generation, also known as the window-to-wall ratio (WWR), of STPVs in the composite climate of India [12] was found to vary with the transparency, orientation, and applied area. Compared to the code-compliant base case model,

the annual energy use of STPV windows is approximately 12% to 21% in hot and humid climates, with larger STPV windows providing greater total annual energy savings [13]. The recommended VLT and WWR of STPV windows in the cold regions of China range from 50% to 60% and 40% to 50%, respectively, thus showing improvements in the energy efficiencies of STPV facades [14]. Ng et al. [15], who examined six commercially available STPV windows in Singapore, found that various design strategies used to optimize the WWR of different photovoltaic modules in varying orientations are necessary to achieve the highest power usage benefits in tropical regions. Compared to the reference glass, medium and large STPV windows in Madrid offered an energy savings potential of 18% to 59% at a VLT of 46.1% [16], whereas in a warm Mediterranean climate with a WWR of 46%, cooling energy accounted for 87% of the reference window energy demand. The addition of STPV windows significantly reduced the cooling load, while the seasonal heating load increased [17]. In Hong Kong, southwest-facing is the best orientation in terms of power generation, and south-facing is the optimal orientation in terms of achieving the best overall energy performance [18], with thermal performance being the top priority for energy savings in the overall system and artificial lighting consumption being secondary [19]. The optimal STPV window design for the semi-arid climate of an Algerian office building included double-glazing photovoltaic modules with a moderate WWR and 20% VLT in the southern facade and 30% VLT toward the east–west axis [20].

The indoor daylight environment during the application of STPV envelopes is also an aspect of this investigation. An STPV integrated with internal daylight shelves is considered an efficient solution to decrease the possibility of glare discomfort [21]. In low-latitude regions, such as Wuhan, Hong Kong, and Kunming, vacuum photovoltaic glass is ranked as the "best" glass product for daylight visual comfort [22]. Fan et al. studied the daylight performance of buildings integrated with STPVs in different climate zones in China [23]. When the useful daylight illumination (UDI) is greater than or equal to 100 lux and less than 2000 lux and when it is daylight for a longer period, it is expected that the daylight comfort to be provided is enhanced. For a cellular office with STPV windows in Nottingham with 30% WWR, the above metrics are 71% and 70% when the VTL values are 20% and 30%, respectively. For the same windows with clear double glazing, the indicator is 56% [24]. In Harbin, Shanghai, and Guangzhou, STPV windows with a VLT of 10% provided improved daylight availability. However, they led to a less uniform distribution of daylight in rooms [25], while the VLT of south-facing BIPV windows is 50% to 70%, which is the optimal range for indoor comfortable daylight in Riyadh, KSA [26].

As one of the most significant factors affecting building energy performance, the innovative construction of STPV envelopes is also the focus of research. Ventilated cavities and inserted encapsulated phase-change materials are considered multi-purpose power-producing facade structures [27]. In an experimental room located in Kovilpatti, Tamil Nadu, India, the transient peak temperature of the STPV module combined with phase-change materials was reduced to 9 °C during the summer, while the energy conversion efficiency was increased by 9.4% [28]. A photovoltaic double-skin facade (PV-DSF) consisting of an outer layer of STPV panels, an inner layer of clear glass windows, and a nonventilated air gap measuring 12 mm wide between the two layers was recommended as an energy-efficient window in cold regions of China [29]. Under winter conditions in cold regions of China, the PV-DSF with an air supply mode was able to reduce net building electricity consumption by 18.5% to 20.2% compared to nonventilated inner loop modes [30]. Lu et al. [31] proposed appropriate operating strategies for ventilated photovoltaic windows consisting of an STPV outer layer, an inner inward-openable window, and a 400 mm airflow cavity under different weather conditions. This research team also evaluated the overall energy performance and energy savings potential of a ventilated PV-DSF with an air gap width between 50 mm and 800 mm in a cool-summer Mediterranean climate zone and determined that the net electricity use was reduced by approximately 50% compared to other commonly used glazing systems in Berkeley, California, USA [32]. They also found that the energy savings potential of the optimized STPV insulating glass unit (IGU)

composed of STPV cells and glass spaced with air layers was 25.3% and 10.7% higher than the energy savings potential of a single clear glass window and a low-emissivity (low-E) glass window, respectively, in Hong Kong [33]. Compared with conventional IGUs, STPV-IGUs achieved energy savings of up to 50% or more in heating-dominated cities such as Harbin, China, and thus, STPV-IGUs with higher light transmittance were recommended [34]. The artificial lighting energy consumption was approximately 431 Wh/day, and the net power generation was 1509 Wh/day for a novel c-Si-based building-integrated STPV-IGU in Berkeley, California, USA [35]. From the same facilities, the mono-crystalline BIPV IGU achieved 16.8% total electricity consumption savings for a room compared to the reference IGU [36]. Data from a single room in New Delhi, India, revealed that the optimum thickness of an STPV thermal Trombe wall should be 0.3 to 0.4 m for thermal load leveling [37].

STPVs were also available for skylights in roofs and shades in addition to windows. In Kovilpatti, India, the PV cell coverage ratio (PVCCR) of skylights was 0.62 with a daylight factor of 4% and 0.72 for an overall energy savings potential of 450 kWh/year [38]. Horizontal photovoltaic overhangs act as window shades to greatly reduce the cooling need in Mediterranean climates, while in hot desert climates, they are less effective than photovoltaic windows [39]. The maximum room temperatures achieved by a building roof-integrated STPV are 22.0 °C and 9.4 °C at an ambient temperature of 4.4 °C in the absence and presence of air cavities, respectively, in the cold climate of Srinagar, India [40]. The optimal installation orientation for solar photovoltaic shades in Hong Kong is south-facing, and the tilt angle is 30° when maximum power generation is targeted. However, considering the overall energy efficiency, a tilt angle of 20° is recommended [41]. In the hot desert climate of Saudi Arabia, the integration of photovoltaic shading devices significantly improved the energy performance and reduced the glare in the room [42].

With respect to the net energy consumption (NEC) of building-integrated STPVs, a comparative analysis must be performed under a variety of climatic conditions. In China, STPVs with higher WWRs exhibited higher energy performance in severely cold, cold, and temperate climates, while the system exhibited the lowest energy potential in hot climates [43]. The annual heating and cooling energy consumption of commercial buildings under six climatic conditions in the United States indicated that the appropriate thermo-optical characteristics of STPV windows vary depending on the climate of the building location. For example, in low and medium latitudes, annual HVAC energy savings of 30% are possible with STPV windows, while at high latitudes, STPVs may be impractical for energy conservation in heating and cooling [44]. In Fortalezait and Florianopolis, Brazil, and Frankfurt, Germany, the use of appropriate control systems reduced the energy consumption of artificial lighting and air conditioning, in addition to generating energy from semitransparent organic solar cells on windows [45]. In Australia, a naturally ventilated perovskite-based PV-DSF achieved total annual energy savings of 34.1%, 86% and 106% in Darwin, Sydney, and Canberra, respectively, compared to conventional technologies [46].

Previous studies have determined that the application strategy of STPVs is closely related to their own performance parameters, design factors in the building integration process, and climatic conditions. More notably, although the solar irradiance on vertical facades is typically half or even less than half of that on roofs, which significantly reduces the power output per unit cell area [47], and integration with roofs does not have the same shading problems as facades [48], STPVs integrated with facades are still studied far more than those integrated with roofs. The main explanation for this phenomenon is that in conventional high-rise buildings, measures related to roofs are not particularly effective in improving the energy efficiency of buildings because roofs represent a small percentage of the envelope area; hence, the space they influence is limited. However, due to the accelerated urbanization in China, in 2021, the Chinese government issued a series of policies to promote BIPVs in towns and strictly control building heights. Therefore,

the study of STPV skylights focusing on energy efficiency is essential for BIPVs with height limitations.

The objective of this paper is to investigate the energy performance of STPV skylights under different climatic conditions and evaluate the energy savings potential based on national mandatory codes that will be implemented soon. Based on the above data, the extent of the impact of each NEC component on the energy savings potential of STPV skylights is explored to provide a reference for the design of BIPVs.

2. Materials and Methods

We investigated the energy savings potential of STPV skylights in China. Five Chinese cities located in different building climate zones (BCZs) and natural daylight climate zones (DCZs) were selected, and the NEC of a room with STPV skylights was simulated using EnergyPlus software according to the variation in skylight design parameters. Furthermore, according to the mandatory standard "General Specification for Energy Conservation and Renewable Energy Utilization in Buildings" being implemented in China in April 2022, the energy consumption limits of buildings in different climate zones were applied as a baseline to calculate the energy efficiencies of STPV skylights and recommend the design parameter thresholds in different zones. Global sensitivity analysis was performed to evaluate the influence of each energy performance component on the energy efficiency of rooms integrated with STPV skylights located in different zones.

2.1. Selected Cities

The applicability of STPVs is influenced not only by the BCZ but also by the DCZ. Hence, it is necessary to consider the BCZ and the DCZ for a given location when assessing building energy performance. There are five primary categories of climate zones in Chinese architectural design, namely, temperate zones, hot summer and warm winter zones, hot summer and cold winter zones, cold zones, and severe cold zones. As well, there are five daylight climate zones (I, II, III, IV, and V) that are identified based on the annual average total illuminance of daylight. All of these constraints are significant in the evaluation of STPV skylights.

DCZ-I has excellent daylight conditions, and the annual average hourly illumination is no less than 45 klx in this zone. The annual average hourly illumination of DCZ-II is less than 45 klx and greater than 40 klx, and that of DCZ-III is less than 40 klx and greater than 35 klx. DCZ-V has the poorest daylight conditions, with an illumination level of less than 30 klx. The daylight conditions of DCZ-IV are better than those of DCZ-V, with an annual average hourly illumination of less than 35 klx and greater than 30 klx. Based on the above context, the five selected cities are Lijiang, Hohhot, Beijing, Guangzhou, and Chongqing. In Table 1, the optimal fixed angles for the maximum annual power generation of STPVs in these five cities are calculated using the PVSYST program. The geographies and climates of the cities considered in this study are presented in Figures 1 and 2.

Table 1. Information on the studied cities.

Cases	City	Longitude (deg.)	Latitude (deg.)	Building Climate Zone	Daylight Climate Zone	Optimal Angle for STPVs (deg.)
Case 1	Lijiang	100.13 E	26.52 N	Temperate	I	29
Case 2	Hohhot	114.41 E	40.49 N	Severe cold	II	38
Case 3	Beijing	116.28 E	39.48 N	Cold	III	37
Case 4	Guangzhou	113.20 E	23.10 N	Hot summer and warm winter	IV	19
Case 5	Chongqing	106.28 E	29.35 N	Hot summer and cold winter	V	18

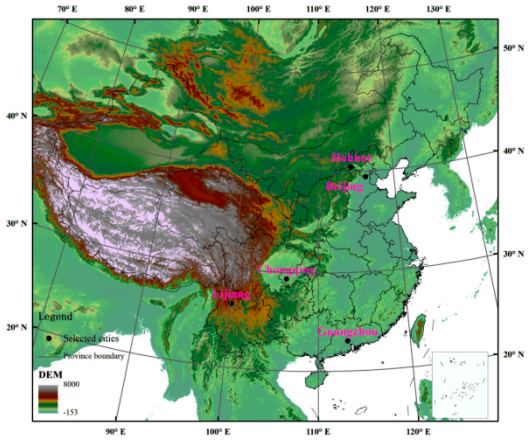

Figure 1. Geographies of the selected cities.

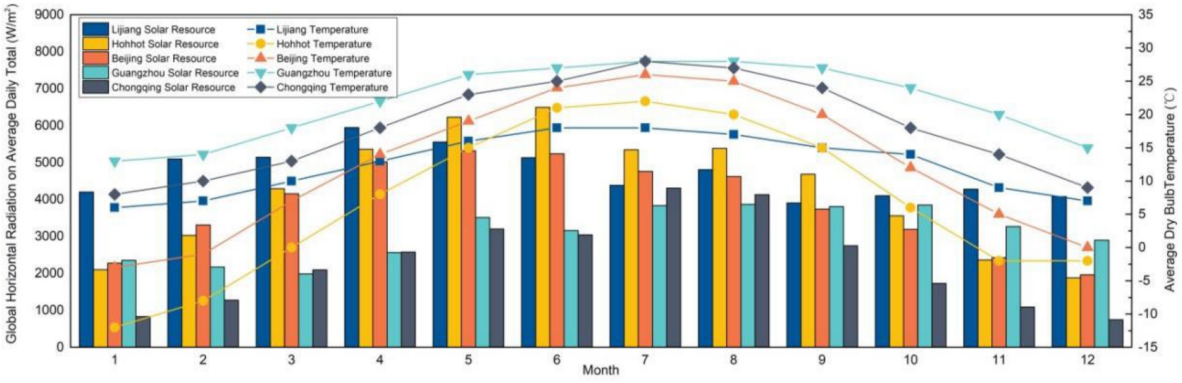

Figure 2. Solar resources and temperatures in the selected cities.

2.2. Geometric Models

The model refers to a square room (8.4 m wide × 8.4 m long × 3.6 m high) given the economy of the column grid design. To discuss the extent to which the STPV skylight design parameters affect the energy savings potential of the space and exclude the influence of non-BIPV parameters, the representative space was placed in the middle of the top floor, with all walls being interior walls (Figure 3). During the simulation, HVAC was also working in surrounding rooms. The skylight-to-roof ratio (SRR) and inclination angle (IA) of STPVs are the primary research variables considered for flat and sloped roofs, respectively. Since the optimal IA of a PV at the study site does not exceed 45°, the SRR and IA distribution intervals range from 10% to 90% and 5° to 45°, respectively.

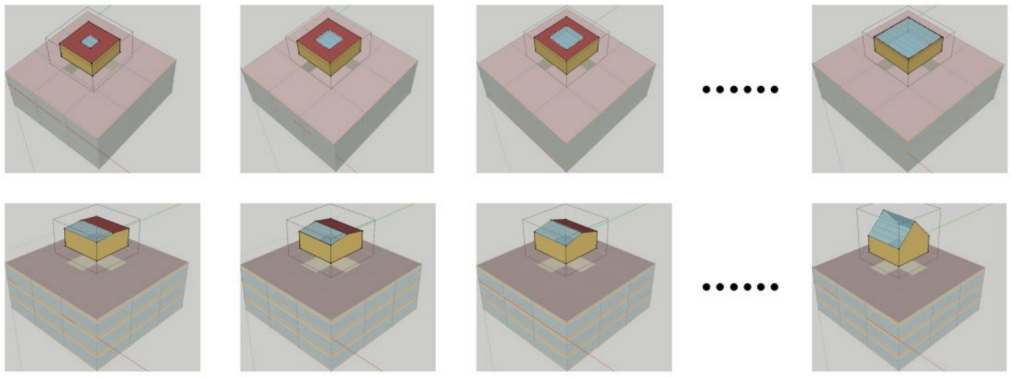

Figure 3. Changing sequences of STPV skylights in the studied room.

2.3. Building Parameters

The building parameters of the energy models are determined based on the "Design standard for the energy efficiency of public buildings" in China released in 2015. The air-conditioning system is assumed to work from 7:00 to 18:00 on weekdays. The thermostat action points for heating and cooling are shown in Figure 4. The floor area per capita is assumed to be 10 m^2 per person.

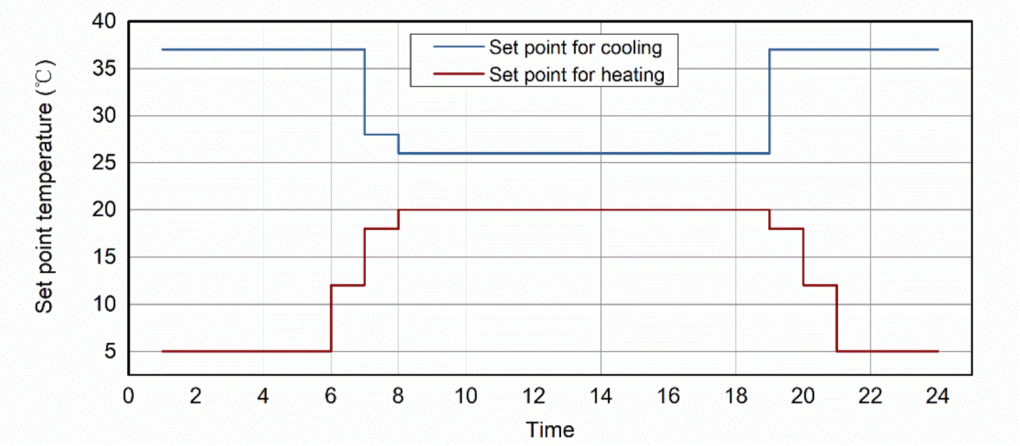

Figure 4. Thermostat action points for heating and cooling.

The STPV skylight module consists of three layers and two air chambers. From the exterior to the interior, the module includes a a-Si-based PV laminated glass with an efficiency of 5.6% [34], a 6 mm air chamber, high-transmittance and low-E glass, a 12 mm air chamber, and clear float glass. The physical properties of PV laminated glass were added to the glass library in Berkeley Lab WINDOW. The optical and thermal parameters of the module were calculated after completing the configuration design. The properties of the photovoltaic and other layers of STPV skylights are presented in Tables 2 and 3. The U-value, solar heat gain coefficient (SHGC), and the visible light transmittance (VLT) of the module are 1.373 W/m^2-K, 0.221 W/m^2-K, and 0.213 W/m^2-K, respectively.

Table 2. Properties of the STPV module.

Electrical Properties	Values	Optical and Thermal Properties	Values
Maximum power, Pm (W)	44	Thickness (m)	0.008
Maximum power voltage, Vm (V)	69	Solar transmittance	0.243
Maximum power current, Im (A)	0.64	Front solar reflectance	0.124
Open circuit voltage, Voc (V)	89	Back solar reflectance	0.379
Short circuit current, Isc (A)	0.77	Visible transmittance	0.284
Fill factor, FF	0.64	Front visible reflectance	0.082
Efficiency, η (%)	5.6	Back visible reflectance	0.379
Temperature coefficient of Isc (%/°C)	0.02	Front emissivity	0.860
Temperature coefficient of Voc (%/°C)	−0.20	Back emissivity	0.850
Temperature coefficient of Pm (%/°C)	−0.19	Conductivity (W/m-K)	0.486

Table 3. Properties of layers of the STPV skylight.

Type	Thickness (m)	Solar Transmittance	Visible Transmittance	Conductivity (W/m-K)
PV laminated glass	0.008	0.243	0.284	0.486
High-transmittance and low-E glass	0.006	0.584	0.817	1
Clear float glass	0.012	0.723	0.87	1

In order to demonstrate the energy benefit of STPV skylights more clearly, based on the specification requirements and the construction form of STPV skylights, and to make the five cases comparable with each other, the reference window consists of 6 mm low-transmission low-E glass, a 12 mm air chamber, 6 mm clear glass, a 12 mm air chamber, and 6 mm clear glass. The U-value, SHGC, and VLT of the reference window are 1.35 W/m^2-K, 0.27, and 0.32, respectively.

2.4. Analysis of the Energy Savings Potential

In this study, a continuous dimming control system was adopted to evaluate the electrical lighting energy use, and two control sensors were located at a height of 0.75 m (representing the height of the working space), with an illuminance level threshold of 450 lx for each sensor (representing the lower limit for task lighting). An ideal heating, ventilation, and air conditioning (HVAC) system was used to calculate the heating and cooling loads. It was assumed that the ideal system can always meet the zone load demands, and the expression air system output $\dot{Q}_{sys}$ in the heat balance is as follows:

$$\dot{Q}_{sys} = C_T C_p \rho_{air} \frac{dT_z}{dt} - \sum_{i=1}^{N_{sl}} \dot{Q}_i - \sum_{i=1}^{N_{surfaces}} h_i A_i (T_{si} - T_z) - \sum_{i=1}^{N_{zones}} \dot{m}_i C_p (T_{zi} - T_z) - \dot{m}_{inf} C_p (T_\infty - T_z) \quad (1)$$

where C_T, C_p, and ρ_{air} are the sensible heat capacity multiplier, zone air specific heat, and zone air density, respectively; and T_z, T_{si}, T_{zi}, and T_∞ are the temperatures of zone air, zone surface, interzone air, and outside air, respectively. $\sum_{i=1}^{N_{sl}} \dot{Q}_i$ represents the sum of the convective internal loads. A_i and h_i are the surface area and convective heat transfer coefficient, respectively, in the process of convective heat transfer from the zone surfaces. $\dot{m}_i$ and $\dot{m}_{inf}$ are the mass flow rates due to interzone air mixing and infiltration of outside air, respectively.

The NEC of buildings with STPV skylights involves cooling energy consumption E_c, heating energy consumption E_h, lighting energy consumption E_l, and power generation E_{pv}. According to the mandatory standard "General Specification for Energy Conservation and Renewable Energy Utilization in Buildings" being implemented in China in April 2022, E_c and E_h are calculated from the simulated cooling load Q_c and heating load Q_h according to the following formula:

$$E_c = \frac{Q_c}{A * COP_c} \quad (2)$$

$$E_h = \frac{Q_h}{A * \eta_h} \quad (3)$$

For these cases, the coefficient of performance for cooling (COP_c) is assumed to be 3.5, and the equivalent heating system efficiency (η_h) is assumed to be 2.18 for severe and cold zones and 2.29 for other zones due to the variation in heating systems, taking into account the geographical differences in China.

The energy savings rate (ESR) is the most intuitive indicator used to evaluate the energy savings potential of a building. The reference used for calculating the ESR is set as the building energy consumption limits for different climate zones, and thus, the values involved in this study are 50 kWh/(m^2·a), 39 kWh/(m^2·a), 36 kWh/(m^2·a), 34 kWh/(m^2·a), and 25 kWh/(m^2·a) for severe cold zones, cold zones, hot summer and cold winter zones, hot summer and warm winter zones, and temperate zones, respectively.

The equation for the ESR is as follows:

$$ESR = \frac{E_{ref} - \left(E_c + E_h + E_l - E_{pv}\right)}{E_{ref}} \quad (4)$$

2.5. Sensitivity Analysis

The global sensitivity analysis method is aimed at measuring the effects of multiple parameters on the output results. In this paper, the Sobol method based on variance

decomposition was selected to evaluate the total effects of the input factors. Sensitivity analysis can be used to determine the changes in outputs due to variances in different input variables. It is assumed that z is the response from an engineering simulation model and is the predicted value for input variable set x. $u(x)$ is a probability distribution function that represents the variations in input variables. Hence, the variance decomposition is formulated as follows [49]:

$$var(E[z|x]) = \sum_{j=1}^{d} V_j + \sum_{1 \le i < j \le d} V_{ij} + \ldots + V_{1,\ldots,d} \quad (5)$$

where d is the number of input variables, j is the j-th input variable, V_j is the variance of the first-order effect for the j-th variable, and V_{ij} is the interaction term for the i-th and j-th inputs. If both sides of this equation are divided by $var(z)$, then the following equation is obtained:

$$\sum_{j=1}^{d} S_j + \sum_{1 \le i \le j \le d} S_{ij} + \ldots + S_{1,\ldots,d} = 1 \quad (6)$$

$$S_j = \frac{V_j}{var(z)} = \frac{var(E[z|x_j])}{var(z)} \quad (7)$$

$$T_j = S_j + S_{1j} + \ldots + S_{1,\ldots,i,\ldots d} = \frac{E[var(z|x_{-j})])}{var(z)} = 1 - \frac{var\left[E(z|x_{-j})\right]}{var(z)} \quad (8)$$

where S_j is the primary effect of the j-th input variable and T_j is the total effect of the j-th input variable. The four input variables are E_c, E_h, E_l, and E_{pv}.

3. Results and Discussion

3.1. Energy Performance

The energy performance of STPV skylights installed on flat and sloped roofs, as displayed in Figures 5 and 6, is analyzed from five subsections: cooling, heating, lighting, power generation, and overall performance.

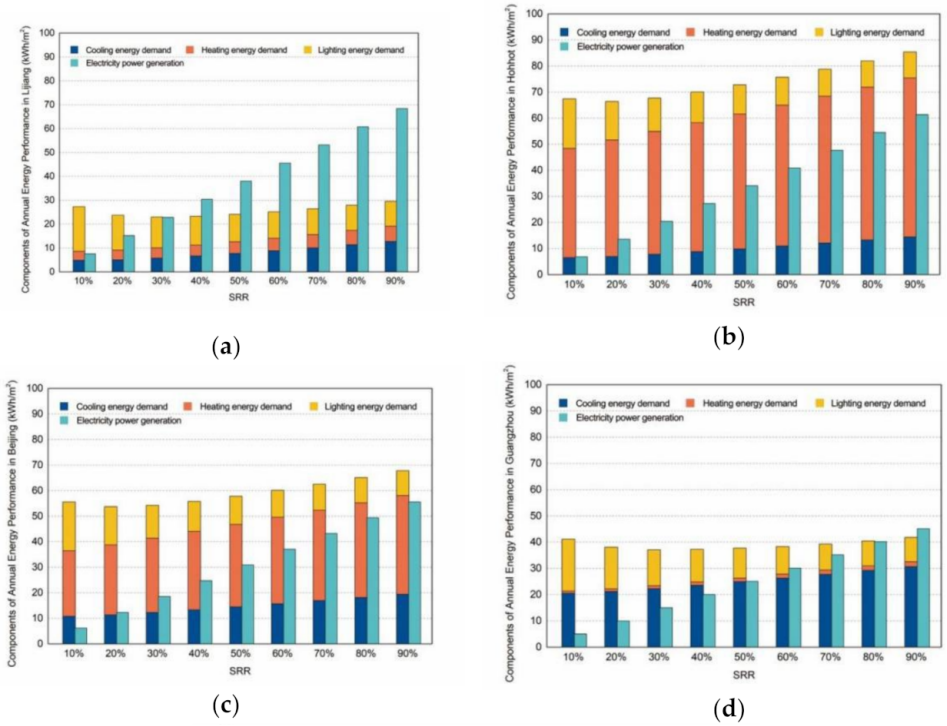

Figure 5. *Cont.*

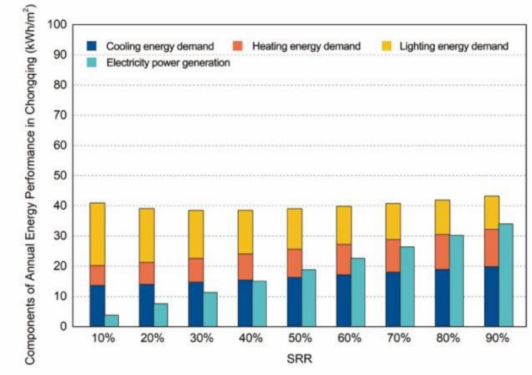

(**e**)

Figure 5. Energy performance of STPV skylights integrated into flat roofs. (**a**) Case 1: Lijiang; (**b**) Case 2: Hohhot; (**c**) Case 3: Beijing; (**d**) Case 4: Guangzhou; (**e**) Case 5: Chongqing.

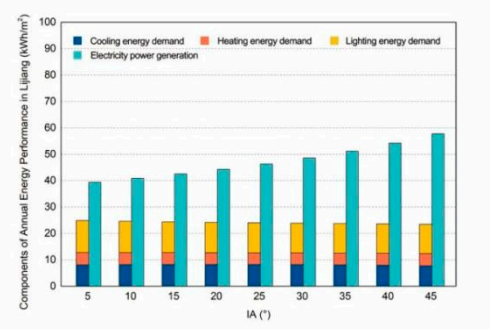

(**a**)

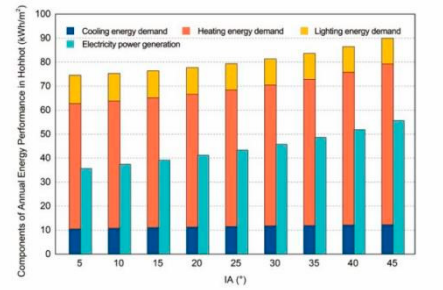

(**b**)

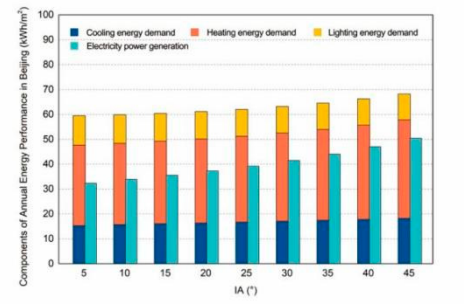

(**c**)

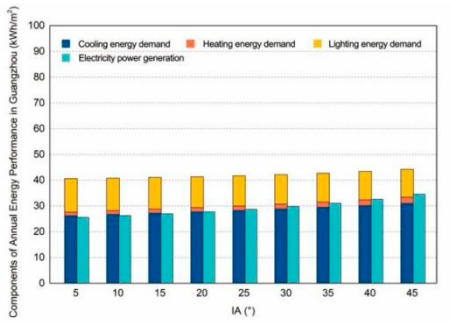

(**d**)

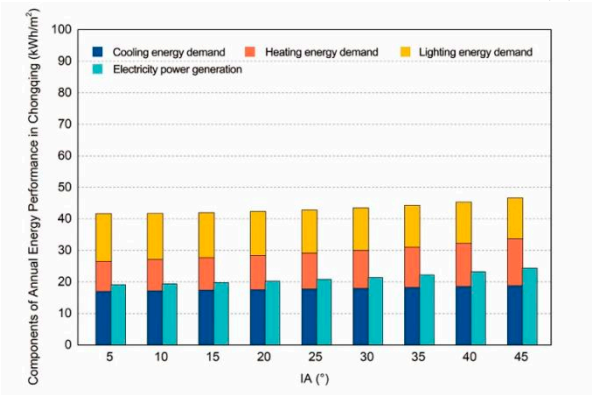

(**e**)

Figure 6. Energy performance of STPV skylights integrated into sloped roofs. (**a**) Case 1: Lijiang; (**b**) Case 2: Hohhot; (**c**) Case 3: Beijing; (**d**) Case 4: Guangzhou; (**e**) Case 5: Chongqing.

3.1.1. Energy Consumption for Cooling and Heating

The cooling energy consumption in Case 1 decreases as the IA increases, while it increases in all other zones. The combined energy consumption for heating and cooling of flat and sloped roofs was at its maximum in Case 2 (cold zone) and at its minimum in Case 1 (temperate region) of the five cases, with annual values of 48.42 to79.29 kWh/m^2 and 8.65 to 19.16 kWh/m^2, respectively. Notably, the larger the SRR is, the narrower the gap.

3.1.2. Lighting Energy Consumption

Lighting energy consumption (LEC) decreases dramatically as the SRR increases from 10% to 30%. Meanwhile, the zones with very excellent (DZ-I), good (DZ-II), and medium (DZ-III) natural daylight environments, corresponding to Case 1, Case 2, and Case 3, respectively, do not differ much in LEC, and as the SRR continues to increase, the gap between the LECs of the three cases gradually widens. The most significant variation in LEC during IA change is observed in the zones with the worst natural daylight conditions.

The magnitude of LEC is not presented exactly according to natural daylight zoning. This is most likely because the daylight zone is classified according to the annual total; thus, some cities have poor annual performance but adequate irradiation for a certain period of time. Coupled with the lower VLT of STPVs, the LEC is related not only to the DCZ but also to the irradiation distribution of each month.

3.1.3. Electricity Power Generation

The electricity power generation (EPG) of STPV systems is directly affected by local solar resources. The results are given in kWh per unit area of room floor (kWh/m^2). When the IA of a sloped roof with STPV skylights is changed, the EPG is related to the local optimal IA for photovoltaic generation, and the area of the STPV skylights changes with the sloped roof angle. The variance becomes increasingly pronounced for large areas of deployed STPVs due to the disparity in solar resources available at each location. When the SRR is 90%, the annual EPGs of the STPV system in the five cases ranged from 34.02 to 68.40 kWh/m^2.

3.1.4. Overall Energy Performance

The net energy consumption (NEC) gradually decreases with increasing SRR when using STPV skylights on flat building roofs. In Case 1 (temperate climate with excellent daylight) and Case 4 (hot summer and warm winter with poor daylight), the NECs of the studied space are both below 0 when the SRRs are no less than 40% and 90%, respectively, which means that the EPGs from the STPV skylight are sufficient to provide the energy needed for heating, cooling, and lighting, but are also sparse. When the SRR reaches 90%, the excess annual power generated by the PV system in the two cases reaches 38.87 kWh and 3.37 kWh per square meter of floor area and is available for other spaces in the building. In other cases, the electricity produced only partially offsets the energy consumption.

The fluctuations in NEC associated with IA changes are not as significant as those related to the SRR. Only the NEC values in Case 1 are always below 0, regardless of the variations in the IA. The NEC values decrease to varying degrees as the IA increases in all cases except for Case 5 (hot summer and cold winter zone with the worst daylight condition), where the NEC is lowest at an IA of 25° for that STPV skylight, although the variations are marginal.

In all cases, the energy consumption of the rooms with STPV skylights is smaller than that of the rooms with reference windows. Figure 7 shows the variation in the difference in energy consumption between rooms with reference windows and rooms with STPV skylights. The sequence of the energy superiority of STPV skylight use in the five cities, from largest to smallest, is consistent with the order of the building's daylight climate zoning, regardless of flat or sloped roofs. The better the solar resource, the more significant the energy benefit of STPV skylight compared to reference skylight. In addition, as SRR and IA increase, the energy advantage of STPV envelopes becomes more obvious. The

results for Case 5 with the best solar resource indicate that STPV skylights save 71.79 kWh per square meter annually compared to reference skylights at an SRR of 90%. The impact of IA variation on STPV energy superiority was not as large as that of SRR.

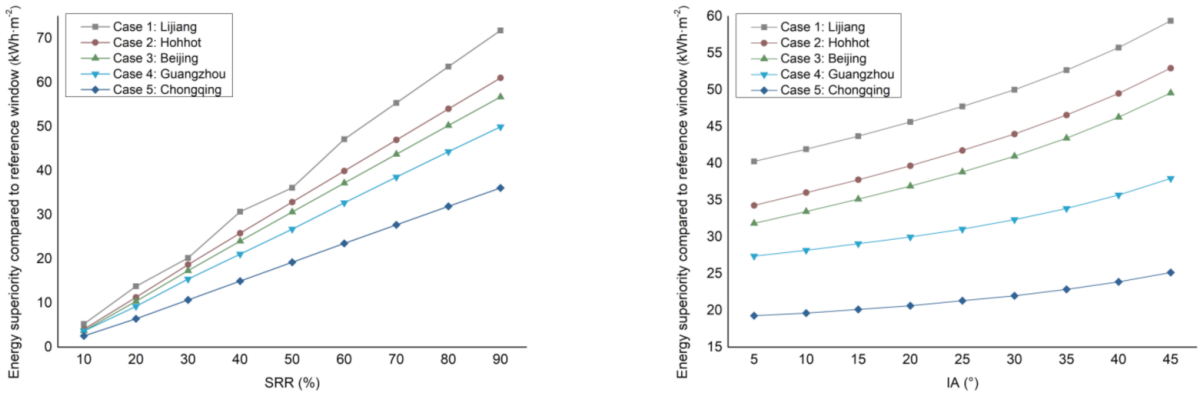

Figure 7. Energy superiority compared to reference window: (**a**) Flat roof; (**b**) Sloped roof.

Overall, building energy performance can be improved by increasing the SRR. The more temperate the climate conditions are, the smaller the SRR required to achieve zero NEC. Therefore, the area of the STPV skylights should be increased as much as possible if the design goal is to achieve zero NEC. Regarding the design of the STPV skylight integrated with the sloped roof, the IA could be decided in Case 5 based on architectural design factors unless the STPV skylight will be used on a large scale and the architect does not have any recommendations for the IA. In other cases, it is feasible to reduce NEC by varying the IA.

3.2. Analysis and Comparison of the Energy Savings Potential

The ESR is the most suitable indicator of the energy efficiency potential of buildings. Energy savings are achievable with an ESR greater than 0 compared to the code requirements. When the above index is greater than 1, a room integrated with STPV skylights is able to ensure the self-sufficiency of energy needs. The energy savings rates of the STPVs are presented in Figure 8.

The ESRs in all cases ranged from −0.27 to 2.55 and increased significantly with the SRR of the STPV skylights. Case 1 has a much higher energy savings potential than the other cases, regardless of the design parameters of the STPV skylight. However, in other cases, with the goal of improving the energy efficiency, the SRR should not be less than 25% in Cases 2 and 3 or 12.5% in Cases 4 and 5. The gap between the ESRs of Case 4 and Case 5 is not significant at an SRR less than 20%, but it does become pronounced as the SRR increases. This is mainly due to Case 4 having slightly better solar resources than Case 5. As the area of the STPV skylights increases, the LEC and EPG increase slightly.

ESR was positively correlated with IA in all cases except Case 5, whose ESR initially increased and reached a maximum as the SRR increased to the range of 25° to 35°, followed by a decline in ESR. Moreover, it exhibited very little fluctuation in ESR compared to the other cases. An increase in the IA leads to an increment in the rate of variation in the ESR for Case 1.

In general, the order of the building baseline energy consumption values in the specifications corresponding to the five cases is basically the same as that of the energy savings potential of STPV skylights on flat roofs. Specifically, the smaller the baseline energy consumption is, the greater the ESR. This could be attributed to the fact that the more temperate the climate is, and the better the natural daylight conditions are, the more pronounced the potential of STPV skylights, as drawbacks such as low VLT are not

exaggerated by the climatic circumstances and the benefits in terms of power generation are more prominent.

With respect to flat roofs, the area used for STPV skylights should be maximized, while for sloped roofs, with the exception of Case 5, the IA is enlarged as much as possible within the range of 0° to 45°. In areas where natural daylight exposure is particularly poor, it is unrealistic to obtain significant improvements in energy efficiency by adjusting the IA of STPV skylights.

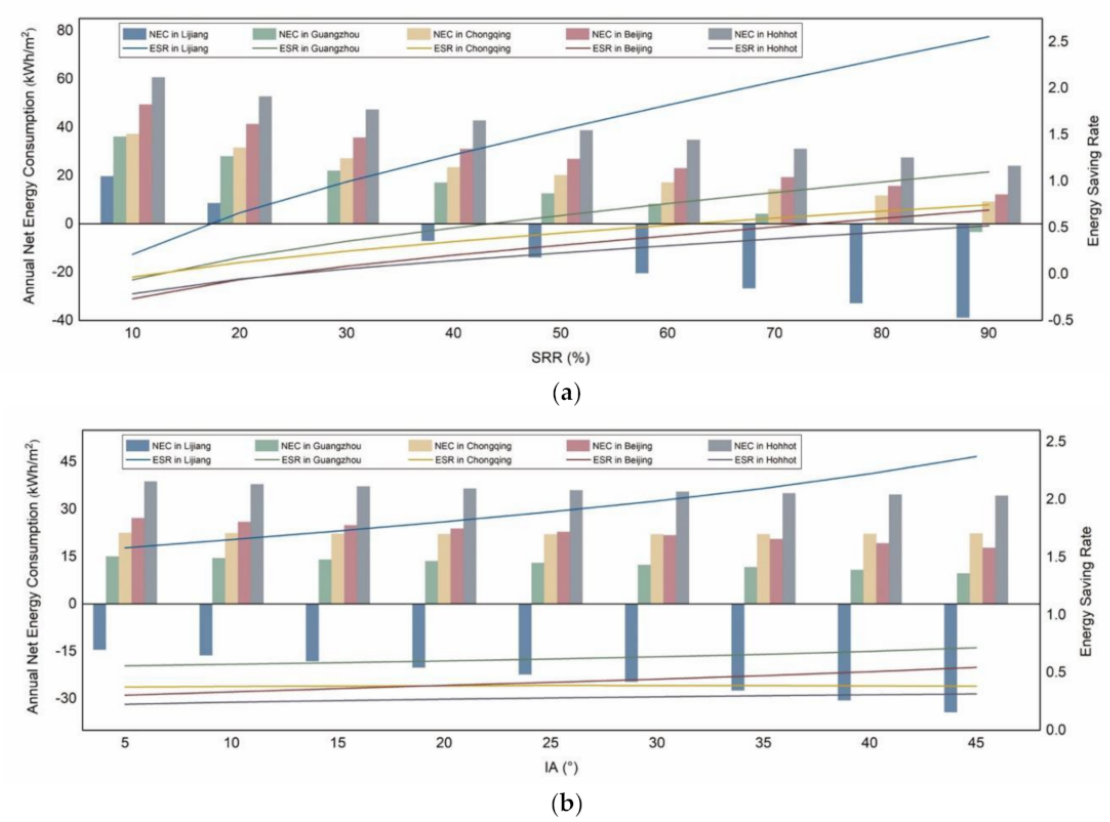

Figure 8. Energy savings rates of buildings integrated with STPV skylights: (**a**) flat roof; (**b**) sloped roof.

3.3. Sensitivity Analysis

The extent to which the variation in the components of NEC affects the ESR with STPV skylights for flat and sloped roofs was evaluated by applying a global sensitivity approach, the results of which are presented in Figures 9 and 10.

EPG is the primary consideration in the design of STVP skylights integrated with flat roofs, mainly because the self-generated electricity of the envelope is a suitable complement to the energy consumption of the building, especially in Case 1, where the energy demand is already quite low, and EPG has an absolutely dominant influence on the energy efficiency of buildings. In severely cold and cold zones (Case 2 and Case 3), as the variation in heating energy consumption caused by the SRR of STPV skylights has a nonnegligible impact on the energy savings rate, more attention should be given to its thermal performance in product selection and skylight construction design. The LEC is more related to the energy savings potential than the other two parts of energy consumption in hot summer and cold winter zones with the poorest natural daylight environment (Case 5). STPV modules with higher VLT or those in combination with conventional glass should be properly considered in the design process.

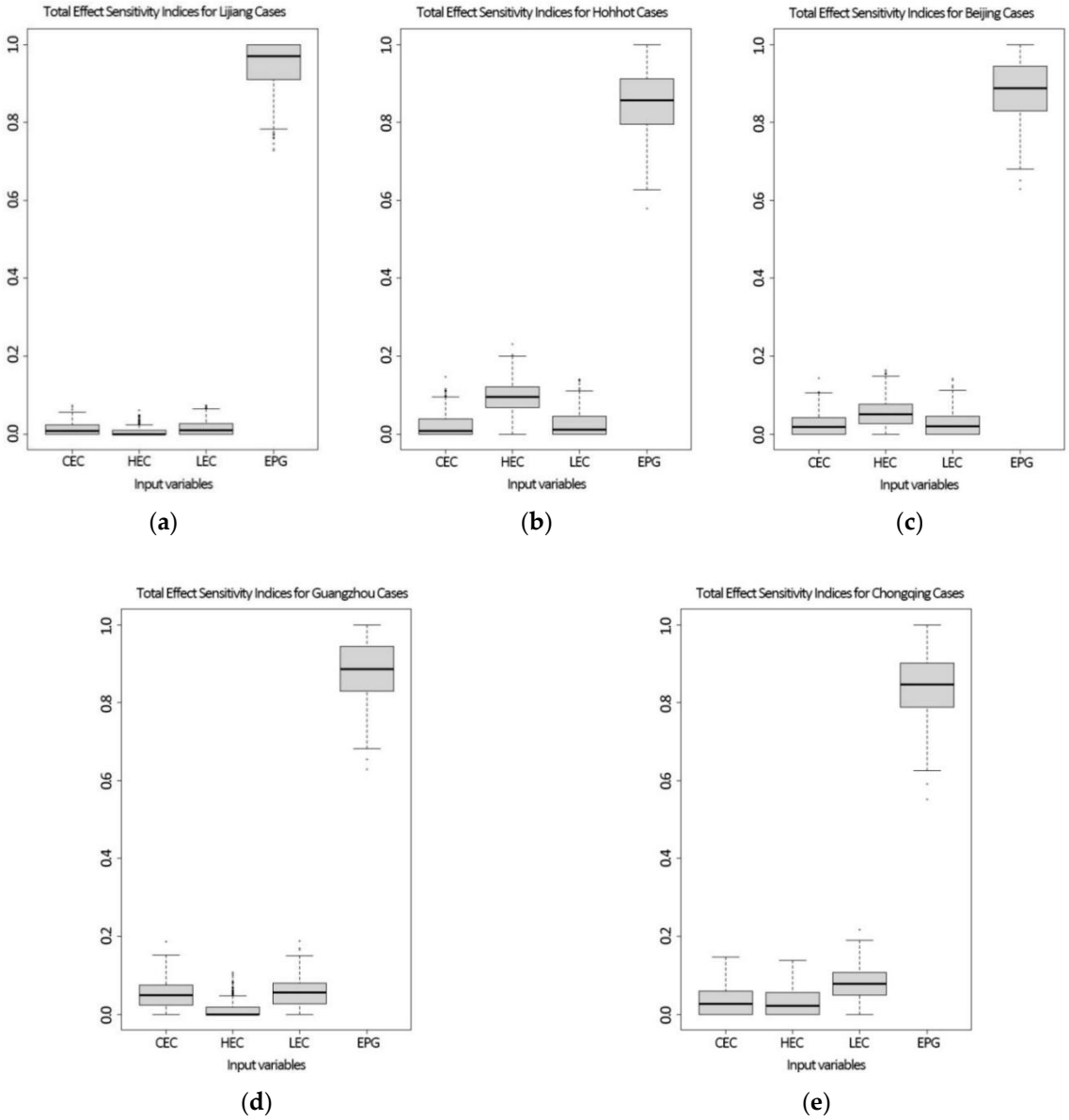

Figure 9. Sensitivity analysis of each component of the STVP energy performance on flat roofs to the ESR. (**a**) Case 1: Lijiang; (**b**) Case 2: Hohhot; (**c**) Case 3: Beijing; (**d**) Case 4: Guangzhou; (**e**) Case 5: Chongqing.

The contribution of EPG to the ESR of STPV skylights on sloped roofs is relatively less than that on flat roofs. In all cases, EPG had the most significant impact on the energy savings potential, except for Case 5, integrated with a sloped roof.

In Case 5 (hot summer and cold winter zone with poor daylight), the most substantial impact on the ESR during the IA variation of the STPV skylight was observed for heating energy consumption and EPG, followed by LEC, while the least was observed for cooling energy consumption. This can be interpreted as a shortcoming of STPV modules with lower VLT values compared to conventional magnified light-transmitting building materials (e.g., glass), and the power generation of the STPV envelope could not produce a noticeable improvement during the varying IA of skylights. However, the alteration in skylight IA causes additional cold air to enter the room through the envelope in winter and expands the volume of space in the room that must be heated. These issues also arise during the cooling period, but the energy savings potential is more sensitive to fluctuations in heating

energy consumption due to external climatic conditions and the efficiency of the energy supply method.

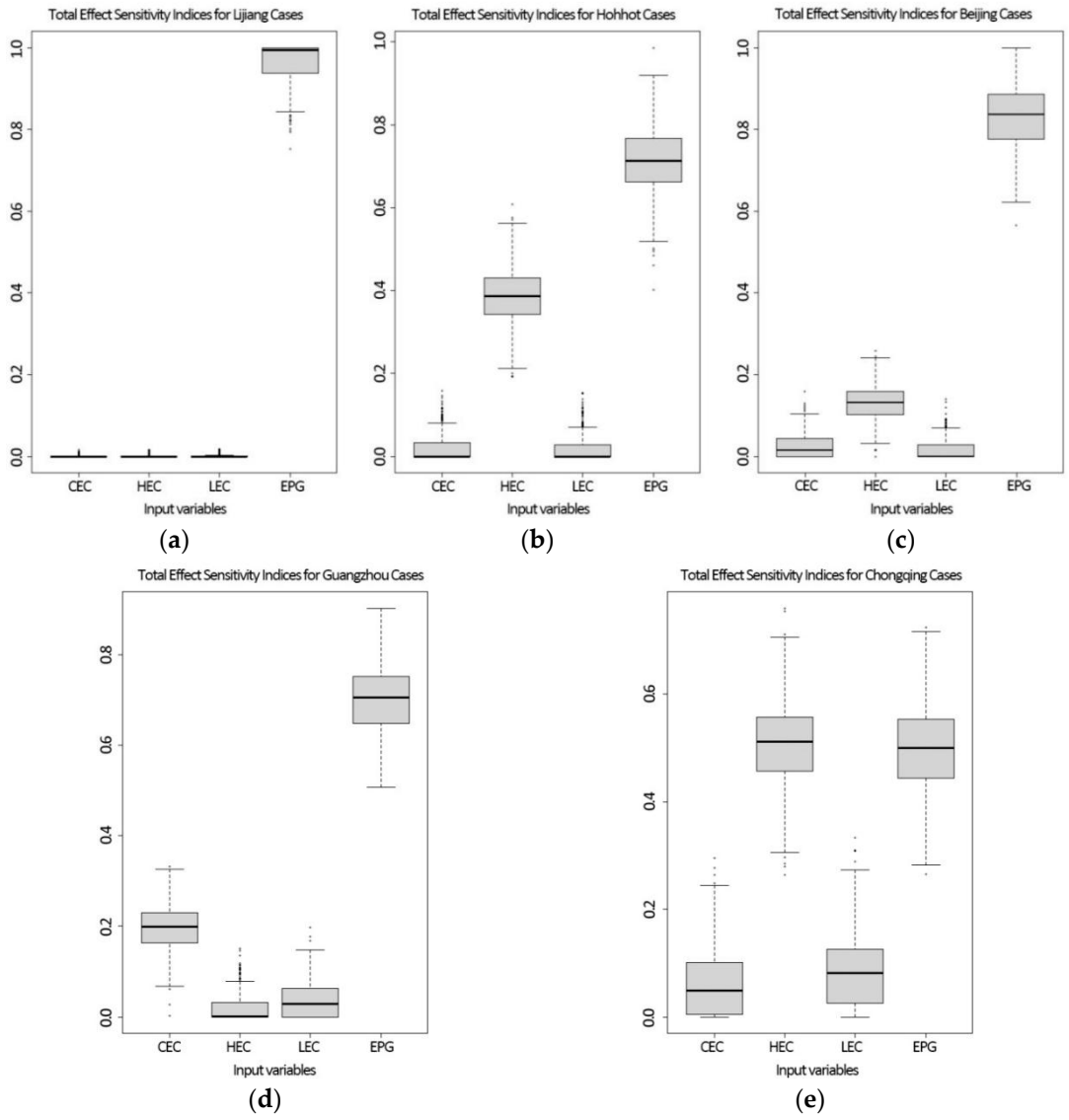

Figure 10. Sensitivity analysis of each component of the STVP energy performance on sloped roofs to the ESR. (**a**) Case 1: Lijiang; (**b**) Case 2: Hohhot; (**c**) Case 3: Beijing; (**d**) Case 4: Guangzhou; (**e**) Case 5: Chongqing.

4. Conclusions

The lower the height of a building, the more limited the area of the envelope available to integrate photovoltaics and the more vital it is to effectively use roofs. In this paper, we investigated the energy performance of STPV skylights and energy superiority compared to a reference window under different climatic conditions, and evaluated the energy savings potential according to the upcoming mandatory national codes. Finally, the extent to which each component of the NEC affects the energy savings potential of STPV skylights was explored. The major findings of this research are as follows.

Regarding the energy performance of STPV skylights, the LEC is related not only to the DCZ but also to the irradiation distribution of each month, and the SRR has a much greater impact on the NEC than does the IA. Furthermore, an NEC below 0 is not possible under all climate conditions. In Cases 1 and 4, the NECs of the studied spaces are below 0 for SRRs of no less than 40% and 90%, respectively.

Regarding the energy savings potential of STPV skylights, taking the code limits as a reference, in temperate zones with excellent daylight conditions, an energy savings potential of 0.21 to 2.55 can be achieved, while the maximum energy savings rate for the other four cases ranges from 0.52 to 1.1. The effect of EPG on the energy savings potential is most pronounced, except for the STPV skylights on sloped roofs in hot summer and cold winter zones with poor daylight, in which a significant influence of heating energy consumption and EPG on ESR is observed during the IA variation of STPV skylights. It is concluded that STPV skylights exhibit promising energy savings potential in China, and this study provides a reference for the design of BIPVs. However, there are some limitations in this study. Only one type of STPV module was selected. Since the higher the VLT of the STPV modules is, the lower the photoelectric conversion efficiency, the suitability of different products in different climate zones may vary. Meanwhile, the impact on the visual comfort of the building interior during the application of various products also varies. Moreover, due to the serious air pollution in some cities, air pollution will have a great impact on the indoor daylight environment and the power generation of building-integrated STPVs. On the other hand, since we focused on the comparison between different models, a detailed design of the STPV system was not performed for all cases. Hence, selecting representative models for STPV circuit design and comparing the differences between experimental data and the theoretical data are key points for future research.

Author Contributions: L.Z., P.W. and Y.H. participated in the whole process of the study; Methodology, W.T.; Writing—review and editing, W.T.; Investigation, Y.S. and B.Y. All authors have read and agreed to the published version of the manuscript.

Funding: The project is funded by Key Research and Development Project in Tianjin [20YFYSGX00020] and Science and Technology Service Network Initiative of Chinese Academy of Sciences [KFJ-STS-QYZD-2021-02-006].

Institutional Review Board Statement: Not applicable.

Informed Consent Statement: Not applicable.

Data Availability Statement: The data that support the findings of this study are available from the corresponding author, upon reasonable request.

Conflicts of Interest: The authors declare no conflict of interest.

References

1. Rounis, E.D.; Athienitis, A.K.; Stathopoulos, T. BIPV/T curtain wall systems: Design, development and testing. *J. Build. Eng.* **2021**, *42*, 103019. [CrossRef]
2. Needell, D.R.; Phelan, M.E.; Hartlove, J.T.; Atwater, H.A. Solar power windows: Connecting scientific advances to market signals. *Energy* **2020**, *219*, 119567. [CrossRef]
3. Saadon, S.; Gaillard, L.; Menezo, C.; Giroux-Julien, S. Exergy, exergoeconomic and enviroeconomic analysis of a building integrated semi-transparent photovoltaic/thermal (BISTPV/T) by natural ventilation. *Renew. Energy* **2019**, *150*, 981–989. [CrossRef]
4. Li, Z.; Zhang, W.; Xie, L.; Wang, W.; Tian, H.; Chen, M.; Li, J. Life cycle assessment of semi-transparent photovoltaic window applied on building. *J. Clean. Prod.* **2021**, *295*, 126403. [CrossRef]
5. Roy, A.; Ghosh, A.; Bhandari, S.; Sundaram, S.; Mallick, T. Perovskite Solar Cells for BIPV Application: A Review. *Buildings* **2020**, *10*, 129. [CrossRef]
6. Khalifeeh, R.; Alrashidi, H.; Sellami, N.; Mallick, T.; Issa, W. State-of-the-Art Review on the Energy Performance of Semi-Transparent Building Integrated Photovoltaic across a Range of Different Climatic and Environmental Conditions. *Energies* **2021**, *14*, 3412. [CrossRef]
7. Singh, D.; Chaudhary, R.; Karthick, A. Review on the progress of building-applied/integrated photovoltaic system. *Environ. Sci. Pollut. Res.* **2021**, *28*, 47689–47724. [CrossRef]
8. Reddy, P.; Gupta, M.V.N.S.; Nundy, S.; Karthick, A.; Ghosh, A. Status of BIPV and BAPV System for Less Energy-Hungry Building in India—A Review. *Appl. Sci.* **2020**, *10*, 2337. [CrossRef]
9. Xu, S.; Liao, W.; Huang, J.; Kang, J. Optimal PV cell coverage ratio for semi-transparent photovoltaics on office building façades in central China. *Energy Build.* **2014**, *77*, 130–138. [CrossRef]
10. Alrashidi, H.; Ghosh, A.; Issa, W.; Sellami, N.; Mallick, T.K.; Sundaram, S. Thermal performance of semitransparent CdTe BIPV window at temperate climate. *Sol. Energy* **2020**, *195*, 536–543. [CrossRef]

11. Chen, F.; Wittkopf, S.K.; Ng, P.K.; Du, H. Solar heat gain coefficient measurement of semi-transparent photovoltaic modules with indoor calorimetric hot box and solar simulator. *Energy Build.* **2012**, *53*, 74–84. [CrossRef]
12. Barman, S.; Chowdhury, A.; Mathur, S.; Mathur, J. Assessment of the efficiency of window integrated CdTe based semi-transparent photovoltaic module. *Sustain. Cities Soc.* **2018**, *37*, 250–262. [CrossRef]
13. Do, S.L.; Shin, M.; Baltazar, J.-C.; Kim, J. Energy benefits from semi-transparent BIPV window and daylight-dimming systems for IECC code-compliance residential buildings in hot and humid climates. *Sol. Energy* **2017**, *155*, 291–303. [CrossRef]
14. Cannavale, A.; Hörantner, M.; Eperon, G.E.; Snaith, H.; Fiorito, F.; Ayr, U.; Martellotta, F. Building integration of semitransparent perovskite-based solar cells: Energy performance and visual comfort assessment. *Appl. Energy* **2017**, *194*, 94–107. [CrossRef]
15. Ng, P.K.; Mithraratne, N.; Kua, H.W. Energy analysis of semi-transparent BIPV in Singapore buildings. *Energy Build.* **2013**, *66*, 274–281. [CrossRef]
16. Olivieri, L.; Caamaño-Martín, E.; Moralejo-Vázquez, F.J.; Martín-Chivelet, N.; Olivieri, F.; Neila-Gonzalez, F.J. Energy saving potential of semi-transparent photovoltaic elements for building integration. *Energy* **2014**, *76*, 572–583. [CrossRef]
17. Skandalos, N.; Karamanis, D. Investigation of thermal performance of semi-transparent PV technologies. *Energy Build.* **2016**, *124*, 19–34. [CrossRef]
18. Zhang, W.; Lu, L.; Peng, J.; Song, A. Comparison of the overall energy performance of semi-transparent photovoltaic windows and common energy-efficient windows in Hong Kong. *Energy Build.* **2016**, *128*, 511–518. [CrossRef]
19. Lu, L.; Law, K.M. Overall energy performance of semi-transparent single-glazed photovoltaic (PV) window for a typical office in Hong Kong. *Renew. Energy* **2013**, *49*, 250–254. [CrossRef]
20. Mesloub, A.; Albaqawy, G.A.; Kandar, M.Z. The Optimum Performance of Building Integrated Photovoltaic (BIPV) Windows Under a Semi-Arid Climate in Algerian Office Buildings. *Sustainability* **2020**, *12*, 1654. [CrossRef]
21. Mesloub, A.; Ghosh, A.; Albaqawy, G.A.; Noaime, E.; Alsolami, B.M. Energy and Daylighting Evaluation of Integrated Semi-transparent Photovoltaic Windows with Internal Light Shelves in Open-Office Buildings. *Adv. Civ. Eng.* **2020**, *2020*, 8867558. [CrossRef]
22. Qiu, C.; Yang, H. Daylighting and overall energy performance of a novel semi-transparent photovoltaic vacuum glazing in different climate zones. *Appl. Energy* **2020**, *276*, 115414. [CrossRef]
23. Fan, Z.; Yang, Z.; Yang, L. Daylight performance assessment of atrium skylight with integrated semi-transparent photovoltaic for different climate zones in China. *Build. Environ.* **2020**, *190*, 107299. [CrossRef]
24. Liu, D.; Sun, Y.; Wilson, R.; Wu, Y. Comprehensive evaluation of window-integrated semi-transparent PV for building daylight performance. *Renew. Energy* **2019**, *145*, 1399–1411. [CrossRef]
25. Sun, Y.; Liu, D.; Flor, J.-F.; Shank, K.; Baig, H.; Wilson, R.; Liu, H.; Sundaram, S.; Mallick, T.K.; Wu, Y. Analysis of the daylight performance of window integrated photovoltaics systems. *Renew. Energy* **2019**, *145*, 153–163. [CrossRef]
26. Ghosh, A.; Mesloub, A.; Touahmia, M.; Ajmi, M. Visual Comfort Analysis of Semi-Transparent Perovskite Based Building Integrated Photovoltaic Window for Hot Desert Climate (Riyadh, Saudi Arabia). *Energies* **2021**, *14*, 1043. [CrossRef]
27. Arkar, C.; Žižak, T.; Domjan, S.; Medved, S. Dynamic parametric models for the holistic evaluation of semi-transparent photovoltaic/thermal façade with latent storage inserts. *Appl. Energy* **2020**, *280*, 115994. [CrossRef]
28. Karthick, A.; Athikesavan, M.M.; Pasupathi, M.; Kumar, N.M.; Chopra, S.; Ghosh, A. Investigation of Inorganic Phase Change Material for a Semi-Transparent Photovoltaic (STPV) Module. *Energies* **2020**, *13*, 3582. [CrossRef]
29. Cheng, Y.; Gao, M.; Jia, J.; Sun, Y.; Fan, Y.; Yu, M. An optimal and comparison study on daylight and overall energy performance of double-glazed photovoltaics windows in cold region of China. *Energy* **2018**, *170*, 356–366. [CrossRef]
30. Jia, J.; Gao, F.; Cheng, Y.; Wang, P.; Ei-Ghetany, H.; Han, J. A comparative study on thermoelectric performances and energy savings of double-skin photovoltaic windows in cold regions of China. *Sol. Energy* **2020**, *206*, 464–472. [CrossRef]
31. Peng, J.; Lu, L.; Yang, H.; Ma, T. Comparative study of the thermal and power performances of a semi-transparent photovoltaic façade under different ventilation modes. *Appl. Energy* **2015**, *138*, 572–583. [CrossRef]
32. Peng, J.; Curcija, D.C.; Lu, L.; Selkowitz, S.E.; Yang, H.; Zhang, W. Numerical investigation of the energy saving potential of a semi-transparent photovoltaic double-skin facade in a cool-summer Mediterranean climate. *Appl. Energy* **2016**, *165*, 345–356. [CrossRef]
33. Wang, M.; Peng, J.; Li, N.; Lu, L.; Ma, T.; Yang, H. Assessment of energy performance of semi-transparent PV insulating glass units using a validated simulation model. *Energy* **2016**, *112*, 538–548. [CrossRef]
34. Zhang, W.; Lu, L. Overall energy assessment of semi-transparent photovoltaic insulated glass units for building integration under different climate conditions. *Renew. Energy* **2018**, *134*, 818–827. [CrossRef]
35. Peng, J.; Curcija, D.C.; Thanachareonkit, A.; Lee, E.S.; Goudey, H.; Selkowitz, S.E. Study on the overall energy performance of a novel c-Si based semitransparent solar photovoltaic window. *Appl. Energy* **2019**, *242*, 854–872. [CrossRef]
36. Peng, J.; Curcija, D.C.; Thanachareonkit, A.; Lee, E.S.; Goudey, H.; Jonsson, J.; Selkowitz, S.E. Comparative study on the overall energy performance between photovoltaic and Low-E insulated glass units. *Sol. Energy* **2020**, *214*, 443–456. [CrossRef]
37. Taffesse, F.; Verma, A.; Singh, S.; Tiwari, G.N. Periodic modeling of semi-transparent photovoltaic thermal-trombe wall (SPVT-TW). *Sol. Energy* **2016**, *135*, 265–273. [CrossRef]
38. Karthick, A.; Murugavel, K.K.; Kalaivani, L. Performance analysis of semitransparent photovoltaic module for skylights. *Energy* **2018**, *162*, 798–812. [CrossRef]

39. Skandalos, N.; Karamanis, D. An optimization approach to photovoltaic building integration towards low energy buildings in different climate zones. *Appl. Energy* **2021**, *295*, 117017. [CrossRef]
40. Vats, K.; Tiwari, G. Performance evaluation of a building integrated semitransparent photovoltaic thermal system for roof and façade. *Energy Build.* **2012**, *45*, 211–218. [CrossRef]
41. Zhang, W.; Lu, L.; Peng, J. Evaluation of potential benefits of solar photovoltaic shadings in Hong Kong. *Energy* **2017**, *137*, 1152–1158. [CrossRef]
42. Mesloub, A.; Ghosh, A.; Touahmia, M.; Albaqawy, G.; Noaime, E.; Alsolami, B. Performance Analysis of Photovoltaic Integrated Shading Devices (PVSDs) and Semi-Transparent Photovoltaic (STPV) Devices Retrofitted to a Prototype Office Building in a Hot Desert Climate. *Sustainability* **2020**, *12*, 10145. [CrossRef]
43. Sun, Y.; Shanks, K.; Baig, H.; Zhang, W.; Hao, X.; Li, Y.; He, B.; Wilson, R.; Liu, H.; Sundaram, S.; et al. Integrated semi-transparent cadmium telluride photovoltaic glazing into windows: Energy and daylight performance for different architecture designs. *Appl. Energy* **2018**, *231*, 972–984. [CrossRef]
44. Chae, Y.T.; Kim, J.; Park, H.; Shin, B. Building energy performance evaluation of building integrated photovoltaic (BIPV) window with semi-transparent solar cells. *Appl. Energy* **2014**, *129*, 217–227. [CrossRef]
45. Leite Didoné, E.; Wagner, A. Semi-transparent PV windows: A study for office buildings in Brazil. *Energy Build.* **2013**, *67*, 136–142. [CrossRef]
46. Yang, S.; Cannavale, A.; Di Carlo, A.; Prasad, D.; Sproul, A.; Fiorito, F. Performance assessment of BIPV/T double-skin façade for various climate zones in Australia: Effects on energy consumption. *Sol. Energy* **2020**, *199*, 377–399. [CrossRef]
47. Barman, S.; Chowdhury, A.; Mathur, S.; Mathur, J. Angular loss of window integrated thin film semi-transparent photovoltaic module. *J. Build. Eng.* **2021**, *40*, 102353. [CrossRef]
48. Yu, G.; Yang, H.; Luo, D.; Cheng, X.; Ansah, M.K. A review on developments and researches of building integrated photovoltaic (BIPV) windows and shading blinds. *Renew. Sustain. Energy Rev.* **2021**, *149*, 111355. [CrossRef]
49. Tian, W.; Yang, S.; Zuo, J.; Li, Z.; Liu, Y. Relationship between built form and energy performance of office buildings in a severe cold Chinese region. *Build. Simul.* **2016**, *10*, 11–24. [CrossRef]